A R C H I V E S O F M E T A L L U R G Y A N D M A T E R I A L S
Volume 50 2005 Issue 2

I.V. ALEXANDROV*, M.V. ZHILINA*, A.V. SCHERBAKOV**, A.I. KORSHUNOV**, P.N. NIZOVTSEV**, A.A. SMOLYAKOV** V.P. SOLOVYEV**, I.J. BEYERLEIN***, R.Z. VALIEV*

FORMATION OF CRYSTALLOGRAPHIC TEXTURE DURING SEVERE PLASTIC DEFORMATION[1)]

FORMOWANIE SIĘ TEKSTURY KRYSTALOGRAFICZNEJ PODCZAS SILNEJ DEFORMACJI PLASTYCZNEJ

The current paper represents the results of recent investigations, aimed at revealing of regularities and establishing of crystallographic texture evolution mechanisms during equal-channel angular pressing (ECAP). Pure Cu was used as material for investigation. The investigations were conducted with the help of computer simulation. The variable parameter was the friction coefficient. Accumulated strain fields, as well as strain rate gradients, were calculated using the variation-difference method (VDM) and the simplest isotropic material model. The strain rate gradients from the VDM program served as input parameters for the viscous-plastic self-consistent model (VPSC), simulating the texture formation processes. Results of modeling are compared to experimental texture measurements.

W pracy przedstawiono wyniki najnowszych badań dotyczących prawidłowości mechanizmu formowania się tekstury krystalograficznej czystej miedzi podczas wyciskania w kanale kątowym (ECAP). Parametrem zmiennym był współczynnik tarcia. Badania wsparto symulacją komputerową.

Za pomocą metody wariacyjno-różniczkowej (VDM) oraz uproszczonego modelu materiału izotropowego obliczono skumulowane pola odkształceń i gradienty prędkości odkształcenia. Gradienty prędkości odkształcenia z programu VDM posłużyły jako parametry wejściowe dla samouzgodnionego, visko- plastycznego modelu (VPSC) symulującego proces formowania się tekstury. Wyniki modelowania porównano z doświadczalnymi pomiarami tekstury.

* UFA STATE AVIATION TECHNICAL UNIVERSITY, 12 K MARX ST., 450000, UFA, RUSSIA

** FEDERAL STATE UNITARY ORGANOZATION "RUSSIAN FEDERAL NUCLEAR CENTER-ALL-RUSSIAN SRI OF EXPERIMENTAL PHYSICS", SAROV, RUSSIA

*** THEORETICAL DIVISION, LOS ALAMOS NATIONAL LABORATORY, LOS ALAMOS, NM 87545

1) invited lecture

1. Introduction

Numerous recent investigations have successfully demonstrated the unique potential of the severe plastic deformation (SPD) technique for the formation of ultra-fine grained (UFG) and nanostructured materials in bulk form of different metals and alloys [1]. However the process of SPD is accompanied by the formation of significant crystallographic texture [2, 3]. Studying of texture is very useful for understanding of SPD deformation mechanisms during processing, structural refinement, and anisotropy in mechanical properties.

Pilot experimental studies, aimed at studying texture evolution, are presented in papers [2, 4, 5, 6, and 7]. These investigations revealed that crystallographic textures, which are formed in pure Cu at room temperature during equal channel angular pressing (ECAP), are rather complicated and asymmetrical.

To analyze the received pole figures (PFs) it was proposed that the ECAP PFs were rotated by some angle in respect to the horizontal axis [4, 5]. As a result the symmetrized PFs corresponded to those formed during rolling, simplifying the analysis. Authors [6, 8] analyzed Cu experimental PFs after the 1st ECAP pass at room temperature in the die-set with angles of channels' intersection of $\Phi = 90°$ [6, 8] and 120° [8]. When analyzing the received PFs, symmetrization was performed in [8] by tilting of the PFs with respect to their horizontal axis. These tilting angles corresponded to angles between the shear plane and the cross section of the deformed billet. In [8], it was found that this tilt angle in textures varied across the sample thickness. In both works [6, 8], PFs were characterized by comparing them with ideal orientations {111}<110>, {111}<112>, {112}<110> and {001}<110>, associated with simple shear textures [9]. L a t e r, authors [7] identified two sources for the inclination in unsymmetrized ECAE textures: one due to Φ and the other due to the deviation of deformation from simple shear. In [7], the orientations found in ECAE textures were rigorously related to those found in simple shear. According to [3], an increase in strain due to the increasing number of passes practically does not change the type of texture, which is formed in Cu during ECAP. However, at the same time the sharpness of texture maxima is growing.

Texture formation during ECAP of Cu at room temperature was studied in papers [6, 10] in great detail. These works compared experimental results with those of modeling, performed in frame of Taylor theory [10] and of the viscous-plastic self-consistent (VPSC) model [9]. Computer simulations of ECAP texture [11] by means of the (VPSC) model [9] proved to be in good qualitative agreement with experimental results in Cu [10, 12, 13], Al and Ni [12, 14]. It was revealed that the experimental PF (111) in the case of FCC Ni is characterized by a concentration of orientations in the direction perpendicular to the shear plane, and also around the shear plane [14]. This situation is characteristic of shear straining in FCC metals. The experimental PF (111) in the case of Al after the 1st pass of ECAP is rather similar to the corresponding PF (111) in Ni, but less symmetric, due to the influence of initial texture of Al [14]. The VPSC model is also used in combination with analytical expressions

[17] taking into account the peculiar features of the material flow, as predicted by slip line theory [15] or FEM [16]. In fact, it becomes possible to predict the evolution of crystallographic texture considering the complex geometry of the material flow that takes place while the billet is pressed through the ECAP die-set [17]. A better agreement between experimental and modeled textures can be achieved if the evolution of tensor components of the strain rate gradient estimated using the 3D finite-element method (FEM) [18] or the 3D variation-difference method (VDM) [19] is taken into account.

The current paper presents the results of recent investigations, aimed at revealing crystallographic texture evolution mechanisms during SPD, performed by means of 3D simulations of ECAP. Simulation results, including the influence of the friction coefficient on the character and homogeneity of crystallographic texture, formed in the bulk Cu billet during 1 ECAP pass are presented.

2. Modeling and experimentel technique

Modeling of the crystallographic texture was conducted using the VPSC model jointly with 3D VDM, which is similar to the FEM method.

To model the process of ECAP by VDM, we used the software DRAKON. DRAKON determines the stress-strain state of elements, taking into account physical and geometrical non-linearity and contact interaction during intense mechanical and thermal loadings in 2D and 3D dimensional states [19].

$$P = P_c + P_T = \frac{\rho_O C_O^2}{n}(\eta^n - 1) + \rho E_T, E_T = E - E_c, \eta = \frac{\rho}{\rho_O}, \quad (1)$$

where P is the overall pressure in the calculated cell, P_c is the cold constituent of pressure, P_T is thermal constituent of pressure, ρ is the density, ρ_o is the initial density; C_0 is the initial space sound velocity; Γ is the Gruneisen coefficient, which was assigned as constant; E_c, E_T are the cold and thermal constituents of specific (per unit mass) internal energy E. The expression for the elastic constituent of internal energy is as follows

$$E_c = \int P_c \frac{d\eta}{\eta^2}, \quad (2)$$

The parameters values in (1) were as follows: ρ_o = 8.96g/cm^3, C_0 = 3.889km/sec, n = 4.3, Γ = 1.96. It was assumed that initially the pressure and the internal energy were equal to zero. The deviatoric components of the stress tensor were determined by the differential theory of thermoplasticity with isotropic hardening. The shear modulus G was found according to the following formula

$$G = \frac{3(1-2\nu)}{2(1+\nu)}\rho C_B^2, \quad (3)$$

where: $C_B^2 = \left(\frac{\partial P}{\partial \rho}\right)_S$ is the sound velocity in the compressed state. The Poisson coefficient was assumed to be constant and equal to $\nu = 0.34$. For the calculations the experimental stress-strain plot was used.

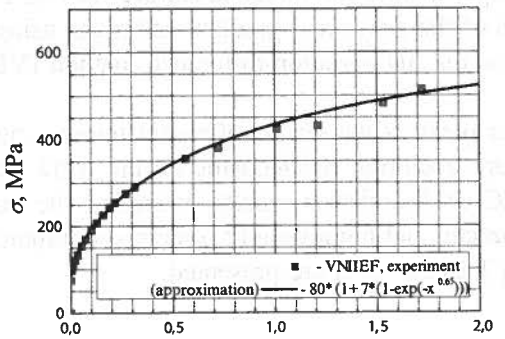

Fig. 1. Plot of Cu straining. Tensile deformation. Room temperature

The problem was assigned for the DRAKON calculations in the following way: material — Cu (99.9%); geometry of the sample — square section rod 8×8 mm^2, 60 mm long; ECAP angle Φ of 90°. The channel walls were assigned as rigid ones. ECAP deformation rate was 6 mm/sec, at room temperature condition.

In the calculations the constitutive law was described by the simplest model of isotropic straining. This was determined with the help of the equation of state in a form of the Gruneisen relation.

The received data for the gradient components of strain rate tensor, the level of the accumulated strain rate and the angle of rotation of the control area for each ECAP step, were used as input data for the modeling of crystallographic texture evolution.

Texture simulations were conducted assuming the external and internal radii of die curvature $r_1 = r_2 = 0$ mm and the friction coefficients as f=0.02 and f=0.12.

In employing the VPSC model, the slip systems {111}<110> were assumed to be active with equal and constant critical resolved shear stresses. Grain interaction and individual relative sizes and orientations of grains were also taken into account, as well as the strain hardening of texture formation process (Voce model [11, 20]). The calculation of the texture when the billet is passing through the die-set was carried out after every stage of VDM, which has been taken for increment of $\Delta t \approx 0.005$ s.

The analysis of texture evolution was carried out of six areas (A1 to A6) (Fig. 2). The position of the areas A3, A5, A6 has been chosen in such a way that one can expect a change in the texture evolution in these areas due to friction.

The initial texture (Fig. 3) has been measured using the X-ray device DRON-3M with an angular interval of 0°-65°, azimuthal interval of 0°-360° in step of 5° for both.

The texture has been represented by 830 separate orientations with specific volume fractions used as input data to start modeling.

The results of modeling were represented in the form of complete (111) PFs. The software "LaboTex" has been applied to calculate the PFs [21].

Modeling results were compared to the corresponding experimental measurements. Experimental studies of crystallographic texture were conducted by means of the X-ray structural analysis method (XRSA) by means of the diffractometer Philips X'Pert system equipped with the texture goniometer ATC- 3.

3. Computer simulation results

3.1. Texture evolution in the center part of the cross sectioned billet (point Al.)

Investigations of texture evolution in the geometrical center of the billet were conducted for the case: $r_1 = r_2 = 0$ mm and friction coefficient f=0.02.

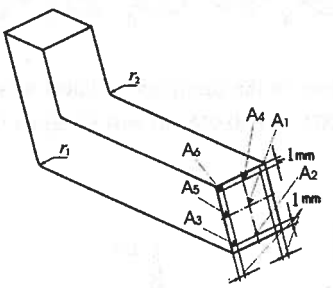

Fig. 2. Location of control areas in the billet

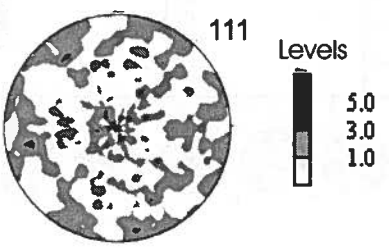

Fig. 3. PF (111) of initial Cu texture

The initial texture of Cu is nearly random and is characterized by some asymmetry in the distribution of texture maxima (Fig. 3).

The evolution of the strain rate gradient tensor components L_{ij} and the PFs are presented in Fig. 4. One can see that the first considerable change in L_{ij} takes place when the control area reaches the zone close to the plane of the channels intersection

(Fig. 4 (c)). Here, the magnitudes of the tension L_{11} and compression L_{22} components are equal. Moreover, the change of the shear component L_{12} is rather similar to the change of the tension component L_{11}, though somewhat earlier.

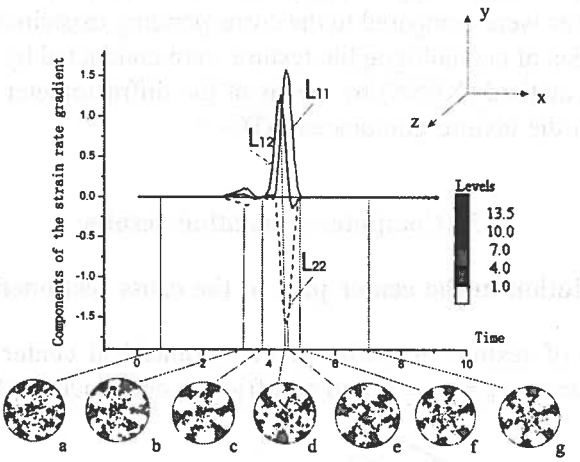

Fig. 4. Dependence of PF (111) view on the strain rate gradient tensor components for control area A1: a) e=0.00036, b) e=0.003, c) e=0.068, d) e=0.31, e) e= 0.6, f) e=1.1, g) e=1.12

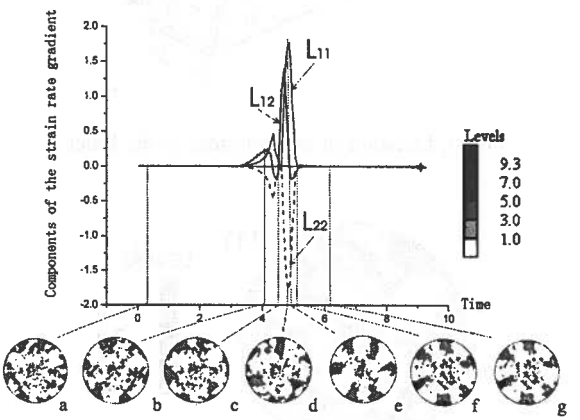

Fig. 5. Dependence of PF (111) view on the strain rate gradient tensor components for control area A4: a) e=0.00038, b) e=0.17, c) e=0.22, d) e=0.37, e) e= 0.75, f) e=1.17, g) e=1.18

As seen from Fig. 4, the formation of crystallographic textures takes place mainly in the zone of intersection of die-set channels (Fig. 4d-e). At the same time, the location of the main texture maxima in PFs, formed in the plane of the channels' intersection

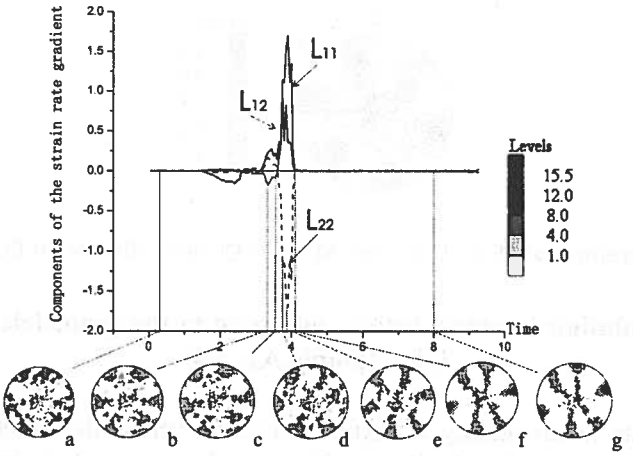

Fig. 6. Dependence of PF (111) view on the strain rate gradient tensor components for control area A2: a) e=0.00031, b) e=0.15, c) e=0.19, d) e=0.21, e) e= 0.34, f) e=0.67, g) e=0.81

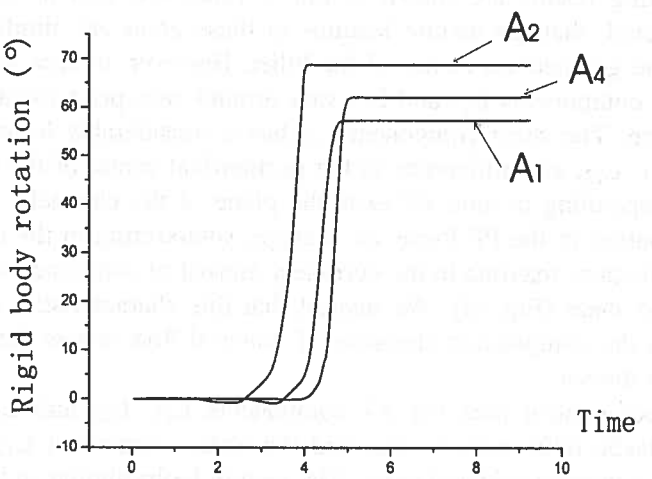

Fig. 7. Values of the rotation angle of the solid body in the die-set for control areas A1, A2 and A4 for the case $r_1 = r_2 = 0$, f=0.02

(Fig. 4d) can be described by a set of orientations typically found in simple shear [7, 9]. Following a material point passing through the area A1, we can see that the general features of the PF do not change significantly, though the location of texture maxima in the periphery of PF becomes more symmetrical, and their intensities sharpen (Fig. 4e-g). The model PF (111), (Fig. 4g) for area A1 when exiting from the zone of the strain accumulation is close to the experimentally received PF (111) of Cu subjected to the first ECAP pass (Fig. 8), considering the rotation of solid body shown in Fig. 7.

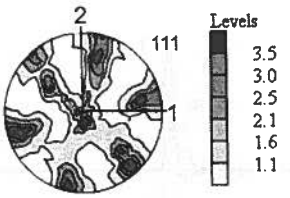

Fig. 8. Experimental PF (111) for area A1 in the Cu billet after the 1st ECAP pass

3.2. Texture evolution in areas, below and above to the geometrical center of the billet (points A2, A4)

To investigate heterogeneity in texture evolution across the billet, we considered two more control areas A2 and A4 (Fig. 2), located respectively below and above the geometrical center of the billet, at a distance of 1 mm from the edge. Investigations were carried out for the following case: $r_1 = r_2 = 0$ mm and a friction coefficient of f=0.12.

The modeling results are shown in Fig. 5 (area A4) and in Fig. 6 (area A2). It should be noted, that the texture features in these areas are similar to the texture developed in the geometrical center of the billet. However, in area A2 the strain rate gradient tensor components L_{11} and L_{22} vary around zero prior to entering the channels' intersection. The shear component L_{12} has a considerably lower value than the components L_{11}, L_{22}, as a difference to the geometrical center of the billet. When the flow line corresponding to area A2 exits the plane of the channels' intersection, the maxima distribution in the PF forms an X-shape, intersecting in the center of the PF. Otherwise, the texture maxima in the periphery consist of components similar to those found in simple shear (Fig. 6f). We suspect that this characteristics of the texture is connected with the complicated character of material flow across the billet along the channels of the die-set.

In the upper control area the A4 components L_{11}, L_{22} and L_{12} vary prior to entering the plastic deformation zone, and the shear component L_{12} has the largest value among the three considered cases. The texture looks similar to that developed in the geometrical center of the billet. The level of the accumulated strain is the largest compared to all the investigated areas; it reaches a value of e=1.18 (Fig. 5g).

The rotation angles as calculated by VDM of material points traveling through areas A2, and A4 are presented in the plot of Fig. 7 too. As it is seen from Fig. 7, the highest rotation angle is observed for control area A2, the lowest — for A1.

3.3. Influence of the friction coefficient in the die-set on the texture evolution

In order to investigate the influence of the friction coefficient on the character of texture formation during the 1st ECAP pass, the friction coefficient was chosen equal to f=0.12, and the parameters of the die-set were chosen as: $r_1 = r_2 = 0$ mm.

The modeling results for texture formation evolution during 1st ECAP pass shows that changes in the friction coefficient did not significantly influence the character of the texture in the geometrical center of the billet (control area A1, Fig. 9). Model PF (111) is close to the experimental PF (Fig. 9) as regards to location of main texture maxima as in case of friction coefficient f=0.12 (Fig. 9) as well as in case of friction coefficient f=0.02 (Fig. 4)

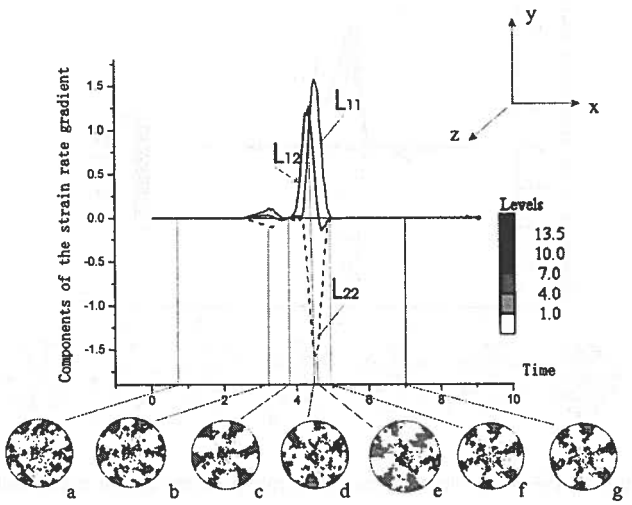

Fig. 9. Dependence of PF (111) view on the strain rate gradient tensor components for control area A1: a) e=0.00036, b) e=0.003, c) e=0.068, d) e=0.31, e) e= 0.6, f) e=1.1, g) e=1.12

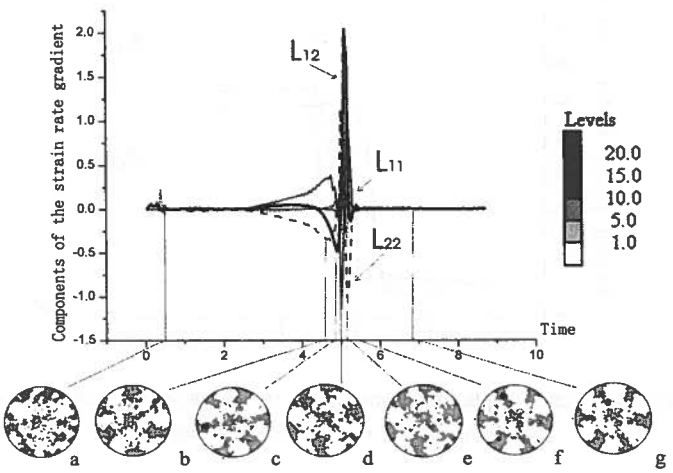

Fig. 10. Dependence of PF (111) view on the strain rate gradient tensor components for control area A4: a) e=0.00038, b) e=0.17, c) e=0.22, d) e=0.37, e) e=0.75, f) e=1.17, g) e=1.18

For the control area A4, located in the upper part of the billet, the view of the PF is similar to the PF for the geometrical center of the billet, except that there is a 30° clockwise tilt of the texture maxima (Fig. 10). Compared to the case in which the friction coefficient is f=0.02, the level of intensity of texture maxima is 2 times higher.

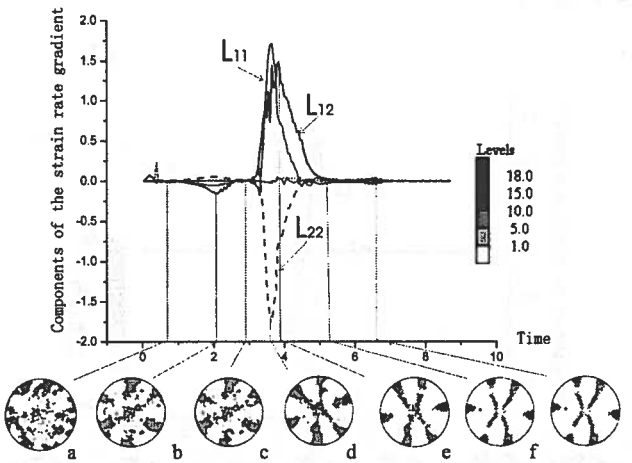

Fig. 11. Dependence of PF (111) view on the strain rate gradient tensor components for control area A2: a) e=0.00031, b) e=0.15, c) e=0.19, d) e=0.21, e) e= 0.34, f) e=0.67, g) e=0.81

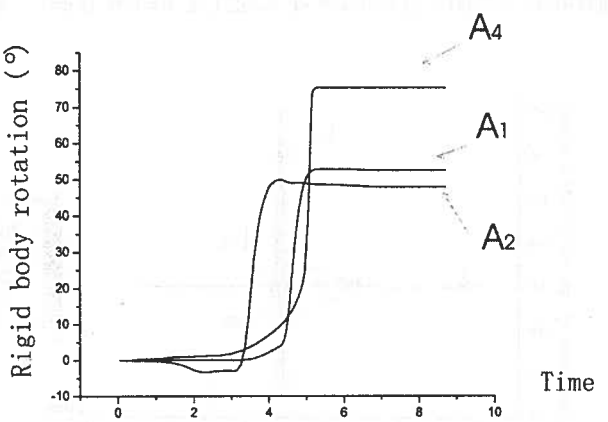

Fig. 12. Values of the rotation angle of the solid body in the die-set for control areas A1, A2 and A4 for the case $r_1 = r_2 = 0$ mm and f=0.12

For the control area A2, located below the geometrical center of the billet the influence of the friction coefficient is more considerable. The X-shaped maxima distribution is observed even in the plane of channels' intersection, where the

shear stresses are maximum (Fig. 11d). With a further displacement of a material point through area A2 the features of the PF are the same, though the texture maxima sharpen with intensity levels of up to 18 and with a simultaneous clockwise rotation by an angle of 30° (Fig. 11e-g). At the same time unlike the case when the friction coefficient is f=0.02, the textures continues to rotate as the material point through area A2 travels in the horizontal channel. Comparing the predictions (Fig. 11) with the available experimental data it should be noted, that the general features of model PFs (111) after the 1st ECAP pass agree best with the case of sharp inner and outer radii, $r_1 = r_2 = 0$ mm, and f=0.12 for control area A2, located at a distance of 1 mm from the bottom side of the billet.

Fig. 12 represents values of rotation angles of the solid body in the die-set for control areas A1, A2, A4 with the friction coefficient of f=0.12. One can see that the rotation is highest for the region A4. However, the rotations in A2 start earlier than in areas A1 and A4. As it is seen, the friction coefficient influences significantly the value of the rotation angle. With the friction coefficient equal to f=0.12, the highest rotation angle corresponds to control are A4, and the lowest one corresponds to A1 (Fig 12). This is in good accordance with the data presented in work [6]. Such a significant influence of the friction coefficient on the value of the rotation angle for control are A4 can be connected either with the fact, that lower layers of the billet during the ECAP process are subjected to the maximal influence of the friction force or with a possible outer angle gap in the die-set.

4. Conclusions

Modeling of the texture formation evolution at the 1st ECAP pass in different areas of the Cu billet showed heterogeneity in the texture evolution, by a degree, which depends on the friction coefficient in the die-set. When comparing the predictions (Fig. 11) with the available experimental data it should be noted, that the general features of model PFs (111) after the 1st ECAP pass agree best with the case of sharp inner and outer radii, $r_1 = r_2 = 0$ mm, and f=0.12 for control area A2, located at a distance of 1 mm from the bottom side of the billet.

The observed differences in intensity levels of main texture maxima for model and experimental PFs can be explained by some choices made when modeling the deformation history by VDM, as well as by the absence of the hardening character when modeling of textures in the VPSC code.

Acknowledgements

The current work was carried out within the framework of project CRDF#10505 Model- driven manufacturing of nanocrystalline structures. The work was also supported by "MMC", OJSC, ETC "Ausferr" and "Intels" Foundation of Science and Education (grant No. 19-04-02).

REFERENCES

[1] R.Z. Valiev, R.K. Islamgaliev, I.V. Alexandrov, Progr. Mater. Sci., **45**, 103-189 (2000).

[2] I.V. Alexandrov, Proceedings of the Eleventh International Conference on Textures of Materials, ICOTOM-11, **2**, 929-940 (1996).

[3] I.V. Alexandrov, A.A. Dubravina, A.R. Kilmametov, V.U. Kazykhanov, R.Z. Valiev, Metals and Materials International **9**, 2, 151-156 (2003).

[4] S.R. Agnew, J.R. Weertman, A progress report in accordance with Agreement, No. C-5689 with the University of California at Berkeley (Los Alamos National Laboratory), August 12 (1996).

[5] J.R. Weertman, S.R Agnew, A progress report for the period 1 to 28 February 1997 (Contract # 7764Q0016-35).

[6] S. Li, I.J. Beyerlein, C.T. Necker, D.J. Alexander, M.A.M. Bourke, Acta Mater. 52, 4859-4875 (2004).

[7] S. Li, I.J. Beyerlein, D.J. Alexander, S.C. Vogel, Acta Mater. **52**, 2111-2125 (2004).

[8] W.H. Huang, L. Chang, P.W. Kao, C.P. Chang, Mater. Sci. Engng., **A 213**, 112-128 (2001).

[9] U.F. Kocks, C.N. Tomé, H.-R. Wenk, Texture and Anisotropy. Preferred Orientations and their Effect on Materials Properties, Cambridge University Press 676, (1998).

[10] I. Kopacz, M. Zehetbauer, L.S. Tóth, I.V. Alexandrov, B. Orther, Proceedings of the 22nanocrystalline alloys structure, properties and modeling. Riso Nat. Lab., Roskilde, Denmark 285-300 (2001).

[11] I. J. Beyerlein, R. Lebensohn, C.N. Tome, Mater. Sci. Eng **A. 345**, 122- 138 (2003).

[12] S.C. Vogel, D.J. Alexander, I.J. Beyerlein, M.A.M. Bourke, D.W. Brown, B. Clausen, C.N. Tomé, R.B. Von Dreele, C. Xu, T.G. Langdon, Mater. Sci. Forum **2661**, 426-432 (2003).

[13] L.S. Tóth, I. Kopacz, M. Zehetbauer, I.V. Alexandrov, in Proc. THERMEC-2000 (Eds.: T. Chandra, et al.), Las Vegas, Dec., on CD (2000).

[14] S.C. Vogel, I.J. Beyerlein, M.A. Bourke, C.N. Tóme, P. Rangaswamy, C. Xu, T.G. Langdon, Mater. Sci. Forum **408-412**, 673-678 (2002).

[15] V.M. Segal, Mat. Sci. Eng **A 345**, 36-46 (2003).

[16] S. Li, M.A.M. Bourke, I.J. Beyerlein, D.J. Alexander, B. Clausen, Mater. Sci. Eng **A. 382/1-2**, 217-236 (2003).

[17] I.J. Beyerlein, C.N. Tomé, Mat. Sci. Engng, **A 380**, 171-190 (2004).

[18] I.N. Budilov, I.V. Alexandrov, Y.V. Lukashuk, I.J. Beyerlein, V.S. Zhernakov, Ultra-fine Grained Materials III TMS Proceeding, NC (USA) 193-198 (2004).

[19] A.I. Abakumov, A.V. Pevnitsky, V.P. Solovyev, IV Zbabakhin Scientific Readings. Proceedings of the International Conference. Snezhinsk, 16- 20 October 227-228 (1995).

[20] C.N. Tomé, G.R. Canova, U.F. Kocks, N. Christodoulou, J.J. Jonas, Acta metall. **32**, 10, 1637-1653 (1984).

[21] K. Pawlik, P. Ozga, LaboTex: The Texture Analysis Software, 'Göttinger Arbeiten zur Geologie und Paläontologie', SB4 (1999).

Received: 21 March 2005.